DETERMINATION BY ELECTROMAGNETIC ANALOG OF THE NORMAL COMPONENT OF INDUCED VELOCITY OF A UNIFORMLY LOADED LIFTING ROTOR WITH SWEPT WAKE OPERATING IN GROUND EFFECT

A THESIS

Presented to

the Faculty of the Graduate Division

by

Robert S. Holmes

In Partial Fulfillment

of the Requirements for the Degree

Master of Science in Aeronautical Engineering

Georgia Institute of Technology

December 1958

3a
12R

DETERMINATION BY ELECTROMAGNETIC ANALOG OF THE NORMAL COMPONENT OF INDUCED VELOCITY OF A UNIFORMLY LOADED LIFTING ROTOR WITH SWEPT WAKE OPERATING IN GROUND EFFECT

Approved:

Walter Castles, Jr.

Robin B. Gray

Thomas W. Jackson

Date approved by Chairman: Dec 9, 1958

"In presenting the dissertation as a partial fulfillment of the requirements for an advanced degree from the Georgia Institute of Technology, I agree that the Library of the Institution shall make it available for inspection and circulation in accordance with its regulations governing materials of this type. I agree that permission to copy from, or to publish from, this dissertation may be granted by the professor under whose direction it was written, or, in his absence, by the dean of the Graduate Division when such copying or publication is solely for scholarly purposes and does not involve potential financial gain. It is understood that any copying from, or publication of, this dissertation which involves potential financial gain will not be allowed without written permission.

______________________ "

ACKNOWLEDGEMENTS

The author wishes to express his appreciation to Professor Walter Castles, Jr. for the suggestion of the topic and for his valuable guidance throughout the preparation of this thesis. Gratitude is also extended to Doctor Thomas W. Jackson and Doctor Robin B. Gray for their review and comments on the material contained herein.

TABLE OF CONTENTS

LIST OF TABLES

LIST OF FIGURES

Page

LIST OF SYMBOLS

C_T	rotor thrust coefficient, $C_T = \dfrac{T}{\rho \pi \Omega^2 R^4}$
MR	output meter reading, decibels
N	subscript for a value at the normalizing point
P	subscript for a value at an arbitrary point P
P_i	induced power in ground effect
P_o	induced power out of ground effect
R	rotor radius
r/R, x	nondimensional radius measured to an arbitrary point from the axis of the rotor
T	rotor thrust
v	normal component of induced velocity at center of the rotor for a semi-infinite length wake, $v = \dfrac{\frac{1}{2}\Omega R C_T}{(1 - 3/2\mu_v^2)(\sqrt{\lambda_v^2 + \mu_v^2})}$
V_i/v	nondimensional normal component of induced velocity at a point, positive downward
Z/R	nondimensional distance of rotor above ground plane
α_v	angle of inclination of rotor with flight path velocity
Γ	circulation strength
λ_v	inflow velocity ratio, $\lambda_v = \dfrac{V \sin\alpha_v - v}{\Omega R}$
μ_v	tip speed ratio, $= \dfrac{V \cos\alpha_v}{\Omega R}$
ρ	mass density, slugs per cubic foot

χ angle of inclination of the wake with the positive normal

ψ azimuth angle of arbitrary point, measured counterclockwise from the downwind position

Ω angular velocity of the rotor

SUMMARY

This report is the result of experiments conducted to determine the normal component of induced velocity of a uniformly loaded lifting rotor with a swept wake and operating in ground effect. An electromagnetic analog in the form of a wire model was utilized and point measurements were made of the magnetic field strength at various points in the flow field about the rotor model and its image.

The actual wake vortex system was approximated by a series of coils representing vortex rings. These coils were placed in juxtaposition so as to simulate the wake of a helicopter operating in forward flight in the lower speed ranges. Measurements were made in the tip path plane of the wake model and its image at points out to four rotor radii from the wake centerline. Image point coordinates were fixed by the rotor height above the ground plane and by the requirements of symmetry.

The values obtained for the wake and its image were added by the principle of superposition to render a total nondimensional velocity ratio for the rotor in ground effect. These velocity ratios were normalized to the point in the rotor plane at the wake centerline.

The results of this study should be useful for estimating the induced velocity distribution about lifting ro-

tors operating at similar wake angles. In addition, the data may be of use in estimating the interference induced velocities of multirotor helicopters and flying platforms. Tables and graphs are presented along with a sample problem.

CHAPTER I

INTRODUCTION

In determining the performance of a lifting rotor, it is necessary to know the magnitude of the induced velocities in the vicinity of the rotor. These velocities are induced by the vortex systems of the rotors. Thus for a multirotor helicopter consideration must be given to those velocities induced by the vortices shed from the other rotors. This study deals with the determination of the normal component of these induced velocities in the flow field as this is the only component which appreciably affects the rotor blade element angles of attack.

The geometry of the wake can be approximated by a vortex system having regular geometric properties. Even for such a simple system, however, mathematical calculations are lengthy. Therefore, use was made in this study of the perfect analogy as developed in Reference 1 between the induced flow field associated with a vortex element immersed in a perfect fluid and that of a magnetic field in space associated with a wire carrying an electric current. An electromagnetic analogy in the form of a wire model was constructed to simulate a wake with angle $\chi = \tan^{-1} 2$, measured between the lower normal to the rotor and the wake axis. The length of the wake model was determined by the height of the rotor above the ground plane. Six nondimensional ground heights Z/R equal to one-half, one, one and one-half, two, three and four rotor radii were chosen. Figure 1 reflects the general arrangement of the analog.

Surveys were made in the plane of the rotor for the primary system or portion of the wake above the ground at azimuth angles ψ of zero, ninety, and one hundred and eighty degrees, measured from the downwind direction. The process was then repeated for the wake image to reproduce the ground effect. Velocity ratios were then added by the principle of superposition and normalized to the center of the rotor.

This analysis assumes that the wake vortex system is a uniform, finite length, elliptic cylinder composed of a large number of circular vortex rings arranged so that the circulation strength per unit length of wake is constant.

A sample problem is included in this paper to demonstrate the application of the experimental and calculated data contained herein. A typical single rotor helicopter at a reasonable ground height and operating in the lower speed range was chosen and the ratio of induced power in ground effect was determined.

CHAPTER II

APPARATUS AND EXPERIMENTAL PROCEDURE

The equipment used for the experimental portion of this study consisted of the following four basic components:

1. The primary coil (wire model of wake vortex system).
2. The secondary coil (search coil).
3. The amplifier and output meter.
4. The power supply.

This equipment was essentially the same as used for the experiments in Reference 2 with the exception that the alternator in the power supply was driven by a synchronous motor.

The procedure used was to measure the voltage induced in the secondary coil by the magnetic field of the alternating current in the primary or wake model coils. Surveys were made in the plane of the rotor of the primary wake system and for corresponding points in the image. Measurements were normalized to the center of the rotor of the primary wake system, and converted to induced velocity ratios as shown in the appendix. These ratios were then added by the principle of superposition to reflect the effect of the ground plane.

The accuracy of the method depends on certain fixed considerations as listed in Reference 2. These include:

1. Extraneous magnetic fields.
2. Impure wave forms in the primary coil circuit.
3. Induced effects in the primary and search coil leads.
4. Search coil dimensions and calibration.
5. Primary-coil field distortion.

Attempts were made in the experimental portion of this study to minimize inaccuracies arising from the sources listed above.

The following is a description of the components utilized in this experiment:

Primary coil (wake model)- The wake model was built up from a series of lumped coils, each wound on a separate Plexiglas ring. The number of rings used in the entire model depended on the wake length which was determined by the height of the rotor above the ground plane. The upper portion of the wake was composed of rings bearing nine turns of No. 17, Brown and Sharpe gage, copper wire. These rings were closely spaced to minimize the distortion in the field due to the lumping of wire turns. Farther down the wake, where the effect of wire turn lumping was negligible, the coils were comprised of rings bearing eighteen turns of wire spaced twice as far apart. All coils were series connected and the input and return wires for each were twisted to minimize the external magnetic fields in the coil leads themselves. The leads from the power supply to the model were also twisted in this manner. All coils had a diameter of twelve inches between wire centers and were spaced along the wake in such a manner as to render a constant number of ampere turns per unit length of wake. The current maintained in the model for all measurements was approximately four amperes. The length of the wake model assembly depended on the nondimensional ground height Z/R and varied from approximately seven inches to fifty-four inches. The coils were mounted on a heavy fiber base with nylon nuts and bolts and were positioned so that the line of coil centers made an angle of 63.45 degrees ($\tan^{-1} 2$) with the negative Z axis. The wake model is as shown in Figures 2 (a) and 2 (b).

Search coil- Due to the fact that the primary-coil field was nonlinear and because point measurements were desired, it was necessary that the search coil dimensions be small compared with the dimensions of the wake model rings. The search coil, which was the same as that used in Reference 1, had a diameter of approximately 0.35 inches to the center of the wire bundle. This bundle had a cross section of square form approximately 0.09 inches on each side and consisted of 1,000 turns of No. 40 Brown and Sharpe gage, copper wire wound on a Plexiglas form. The form itself was mounted on a Plexiglas support and a coaxial cable was used to connect the search coil to the amplifier to minimize any current induced in this portion of the pickup circuit. To facilitate measurements the base of the search coil support and the top of the supporting table were scribed with straight lines spaced at appropriate fractions of the rotor radius. For surveys at the 90 degree azimuth a scribed vertical wooden ramp was used for measurements. As the field strength measurements were normalized to the center of the rotor the necessity for obtaining a separate calibration of the search coil circuit was eliminated. Figure 3 shows the entire search coil assembly together with its coaxial connector.

Amplifier and output meter- The entire pickup circuit included a commercial standing wave indicator in addition to the search coil and coaxial cable mentioned above. This indicator, which had a maximum sensitivity of 0.1 microvolt, consisted of an indicating meter, a high-gain 400 cycle fixed-frequency amplifier with a calibrated gain control covering a 60 decibel range, and a narrow 400 cycle band-pass-filter network which had a sharp cutoff at 400 ± 5 cycles per second. The input impedance of the amplifier was 200,000 ohms which, as indicated in Reference 2, was sufficient to eliminate any calibration of the meter scale. The amplifier was placed in a separate room from the field coils to eliminate any appreciable magnetic coupling from these coils. Figure 4 shows the standing wave indicator with coaxial connector.

Power supply- A synchronous motor drove a 400 cycle aircraft inverter to supply the power to the field coils. Between the inverter and the coils were placed a voltmeter, ammeter, capacitors, and two variable resistors. The capacitors were chosen so as to place the entire circuit in resonance for each different length wake and the resistors were adjusted to provide approximately four amperes in the circuit. Figure 5 shows the power supply which was also located in a room separate from the field coils to reduce magnetic coupling.

Field survey procedure- The primary coil circuit was given a warm-up period of thirty minutes prior to any surveys. Measurements were then made to the normalizing point at the center of the wake in the plane of the rotor for which the nondimensional normal component of induced velocity was calculated using tables of vortex ring strength. The same normalizing point was used throughout the survey. For each nondimensional ground height Z/R, the magnetic field strength was measured at points along a radial line extending from the axis of the wire model to a distance of four rotor radii out. This was accomplished for the angle ψ equal to 0°, 90°, and 180°, measured from the downwind direction. Since the flow is symmetric about the longitudinal axis of the wake, the values obtained for $\psi = 90°$ are the same as those for $\psi = 270°$. The measurements described above were made for each of six nondimensional rotor heights Z/R = 0.5, 1.0, 1.5, 2.0, 3.0, and 4.0.

Reduction of data- The meter readings recorded in the field survey were measured in decibels and thus necessitated a conversion to a velocity ratio using the following formula:

$$\left(\frac{V_i}{V}\right)_P = \left(\frac{V_i}{V}\right)_N \left[\frac{\text{antilog } 0.1\ (MR)_P}{\text{antilog } 0.1\ (MR)_N}\right]$$

where

$\frac{V_i}{v}$ = nondimensional normal component of induced velocity

P = subscript referring the point in space at which measurements are taken

N = subscript referring to the normalizing point for which computed values are known

The method of determination of $\left(\frac{V_i}{v}\right)_N$ is shown in Appendix I. The sign of each value of $\left(\frac{V_i}{v}\right)_P$ was determined by considerations of the flow field, the trends of the data, and observance of the reversal of the trend of meter readings. The results are shown in Table 1 and in Figures 6 and 7.

If it is desired to convert $\frac{V_i}{v}$ as given here to an actual dimensional velocity V_i at a point, use can be made of the approximation from Reference 3 for v that

$$v = \frac{\frac{1}{2}\Omega R C_T}{(1 - 3/2\mu_v^2)\sqrt{\lambda_v^2 + \mu_v^2}}$$

where $\lambda_v = \dfrac{V\sin\alpha_v - v}{\Omega R}$

$\mu_v = \dfrac{V\cos\alpha_v}{\Omega R}$

α_v = angle of attack of the tip path plane

CHAPTER III

RESULTS

Table 1 shows the experimental results where, for each table, $\frac{V_i}{V}$ is recorded for various values of r/R and Z/R. This table contains the superimposed values of $\frac{V_i}{V}$ for the wake and its image. Figures 6 and 7 give a graphical presentation of these results, Figure 6 plotting $\frac{V_i}{V}$ vs r/R for each Z/R and Figure 7 plotting $\frac{V_i}{V}$ vs Z/R for each r/R and azimuth angle ψ.

Table 2 shows the experimental values of $\frac{V_i}{V}$ which are the result of the image only. If the contribution of the primary wake only is desired the values from Tables 1 and 2 can be combined.

Figure 8 is a plot of the ratio of the induced power required in ground effect P_i, to that required out of ground effect P_o. These values are plotted against Z/R for two values of the tip speed ratio μ_v. Appendix II shows the method used in determining this power ratio and Chapter IV provides a sample problem to illustrate the use of this graphical data for the representative helicopter shown in Figure 9.

CHAPTER IV

SAMPLE PROBLEM SHOWING THE DETERMINATION OF INDUCED POWER REQUIRED FOR A HELICOPTER FLYING IN GROUND EFFECT

Given a helicopter of the configuration and dimensions shown in Figure 9. It is desired to find the induced power P_i required for this helicopter operating at various values of the nondimensional ground height Z/R.

Pertinent characteristics for this helicopter are as follows:

Blade tip circle radius $R = 28$ feet

Blade tip speed $\Omega R = 600$ feet per second

Airspeed $V = 40$ miles per hour $= 58.6$ feet per second

Assuming a tip speed ratio μ_v of 0.1 and using the relationship that $\chi = \tan^{-1} 2$, we have

$$\chi = \tan^{-1} \frac{\mu_v}{\lambda_v} \qquad \text{or} \qquad \lambda_v = \tfrac{1}{2}\mu_v = .05$$

and $$C_T = \frac{T}{\rho \pi \Omega^2 R^4} = \frac{12000}{(.002378)\,(\pi)\,(600)^2\,(28)^2}$$

$$= .00568$$

Therefore

$$v = \frac{\frac{1}{2}\Omega R C_T}{(1 - 3/2\,\mu_v^2)} \cdot \frac{1}{\sqrt{\lambda_v^2 + \mu_v^2}} = \frac{(.5)(600)(.00568)}{\left[1 - 3/2(.1)^2\right]\sqrt{.0125}}$$

$$= 15.43 \text{ feet per second.}$$

and P_o, the induced power out of ground effect, can be expressed as

$$P_o = \frac{Tv}{550} = \frac{(12000)(15.43)}{550} = 337 \text{ HP}$$

Figure 8 gives the variation of the induced power ratio with ground height and for the values of Z/R shown in the table below the ratio P_i/P_o can be found from Figure 8 and the value of P_i, the induced power in ground effect, can be determined. These values are listed below.

Z/R	P_i/P_o	P_o	P_i
3.0	0.970	337 HP	327 HP
2.0	0.954	337 HP	321 HP
1.0	0.850	337 HP	286 HP
0.5	0.585	337 HP	197 HP

CHAPTER V

CONCLUSIONS

The accuracy of the experimental data contained in this report is not known. The electromagnetic analogy utilized contains certain inherent inaccuracies and the assumption that the wake of the rotor is a skewed uniform elliptic cylinder of constant sheet strength is an additional source of error. Also, in the determination of the graph of P_i/P_o, numerical integration was utilized, which by itself contains certain inaccuracies.

It is anticipated that the data contained in Tables 1 and 2 will be useful for estimating the interference induced velocities of multirotor helicopters and for determining the approximate induced velocity on the longitudinal and lateral axis of single rotors in ground effect. Figure 8 should be useful for estimating the induced power requirements of helicopters in ground effect.

APPENDICES

APPENDIX I

CALCULATION OF NONDIMENSIONAL NORMAL COMPONENT OF INDUCED VELOCITY AT THE NORMALIZING POINT

In Chapter II of this report it was shown that the nondimensional normal component of induced velocity at a point P is given by

$$\left(\frac{V_i}{v}\right)_P = \left(\frac{V_i}{v}\right)_N \left[\frac{\text{antilog } 0.1(MR)_P}{\text{antilog } 0.1(MR)_N}\right]$$

The value of $\left(\frac{V_i}{v}\right)_N$ used in the above expression was determined by the use of Table 1 in Reference 4 which listed numerical values of the nondimensional normal component of induced velocity in the vicinity of a vortex ring. A finite number of rings was selected for each ground height and the corresponding values of $\frac{v_z R}{\Gamma}$ were added with Γ and R both taken equal to one. This resulted in the normal component of velocity v_z at the center of the rotor. From these values the velocity ratio at the normalizing point can be found by use of

$$\left(\frac{V_i}{v}\right)_N = \frac{(v_z)_N}{\frac{1}{2}d\Gamma/dL}$$

where $\frac{d\Gamma}{dL}$ is the sheet strength per unit length along the wake axis. As each ring had a circulation strength of one unit the value of $\frac{d\Gamma}{dL}$ became a function of the wake angle χ and was easily determined. The values of $\left(\frac{V_i}{v}\right)_N$ are shown to four significant figures in the table below for Z/R = 0.5, 1.0, 1.5, and 2.0.

Z/R	$(V_i/v)_N$
0.5	0.9354
1.0	.9603
1.5	.9531
2.0	.9497

Since the tables mentioned above in Reference 4 extended only to a value of Z/R = 2.45 it was necessary to make use of the relationship from Reference 5 that

$$v_z = \frac{\Gamma}{2\pi r'} \frac{1}{\sqrt{x^2 + (r+1)^2}} \left\{ K(k) - \left[1 + \frac{2(r - 1)}{x^2 + (r - 1)^2} \right] E(k) \right\}$$

where r' = radius of vortex ring

x, r = point coordinates

$K(k)$ = complete elliptic integral of the first kind

$E(k)$ = complete elliptic integral of the second kind

Values of v_z were determined from this expression and added to those for v_z from the tables to determine $(V_i/v)_N$ for Z/R of 3 and 4. These values are shown below.

Z/R	$(V_i/v)_N$
3.0	0.9471
4.0	.9462

The magnitude of the contribution to $(V_i/v)_N$ for values of Z/R beyond .75 is negative, resulting in smaller positive values of $(V_i/v)_N$ as Z/R increases. This occurs to a Z/R of approximately 5, at which point $(V_i/v)_N$ begins to increase to one, the velocity ratio for a semi-infinite wake.

APPENDIX II

DETERMINATION OF INDUCED POWER RATIO $\frac{P_i}{P_o}$

This appendix is devoted to a brief explanation of the method employed in the determination of Figure 8 which shows the ratio of induced power in ground effect to that out of ground effect vs nondimensional ground height Z/R.

Reference 3 shows that the circulation strength Γ for a blade at angle ψ can be expressed by the relation:

$$\Gamma = \frac{2\pi \Omega R^2 C_T}{b(1 - 3/2\mu_v^2)} \left[1 - 3/2\mu_v \sin\psi\right] \qquad (1)$$

Also, an increment of thrust on a blade element can be represented as

$$dT = \rho \Gamma U \cos \phi_v \, dr \qquad (2)$$

where U is the resultant velocity at angle ϕ_v with the blade element. Then

$$U\cos\phi_v = \left[\Omega R\right]\left[X + \mu_v \sin\psi\right] \qquad (3)$$

where $x = r/R$. However,

$$dP_i = dT \cdot V_i$$

where dP_i is the induced power required by the blade element located at radius r and azimuth angle ψ. Therefore

$$dP_i = \frac{2\rho\pi\Omega R^2 C_T}{b(1 - 3/2\mu_v^2)}\left[1 - 3/2\mu_v \sin\psi\right]\left[\Omega R\right]\left[X + \mu_v \sin\psi\right]V_i dr \quad (4)$$

and since P_o, the induced power required for the whole rotor out of ground effect can be expressed as

$$P_o = Tv = \rho\pi\Omega^2 R^4 C_T v \quad (5)$$

then it follows that the induced power ratio for a blade at a particular azimuth angle ψ is

$$\left(\frac{P_i}{P_o}\right)_\psi = \frac{2(1 - 3/2\mu_v \sin\psi)}{R(1 - 3/2\mu_v^2)}\int_0^R (r/R + \mu_v \sin\psi)V_i/v \cdot dr \quad (6)$$

and since $r/R = x$, it follows that

$$\left(\frac{P_i}{P_o}\right)_\psi = \frac{2(1 - 3/2\mu_v \sin\psi)}{1 - 3/2\mu_v^2}\int_0^1 (X + \mu_v \sin\psi)\frac{V_i}{v}\, dX \quad (7)$$

Values of the nondimensional normal component of induced velocity V_i/v for each ψ and x are as given in Table 1 of this report. The total ratio P_i/P_o was determined for each ground height and blade azimuth angles of 0, 90, 180, 270, and 360 degrees by integration of expression 7 above using Simpson's Rule for numerical integration with ten increments of radius. The final ratio for the entire 360 degrees of blade travel was then determined by again using Simpson's Rule with the four increments of azimuth angle ψ. These induced power ratios were computed for values of μ_v of 0.04

and 0.10 and are shown in Figure 8 as a plot against Z/R.

r/R	V_i/v for values of Z/R of -					
	½	1	1½	2	3	4
0	0.477	0.816	0.883	0.912	0.930	0.937
0.2	.434	.849	.965	.998	1.019	1.006
0.4	.430	.953	1.068	1.134	1.147	1.132
0.6	.520	1.075	1.247	1.303	1.341	1.294
0.8	.763	1.313	1.525	1.590	1.618	1.625
0.9	1.066	1.624	1.870	1.922	1.968	1.959
1.1	.050	.510	.832	.901	.970	.952
1.2	.079	.610	.849	.942	.992	.988
1.6	-.177	.230	.518	.632	.685	.694
2.0	-.109	.034	.300	.439	.509	.516
2.4	-.070	-.057	.140	.299	.384	.395
2.8	-.036	-.079	.046	.190	.283	.305
3.2	-.018	-.056	-.017	.111	.222	.246
3.6	-.013	-.039	-.040	.049	.167	.197
4.0	-.008	-.012	-.019	.006	.121	.158

Table 1 (a) - Nondimensional Values of Normal Component of Induced Velocity V_i/v at Azimuth Angle $\Psi = 0°$ In Plane of a Lifting Rotor For Which $\chi = \tan^{-1} 2$ (63.45°).

r/R	V_i/v for values of Z/R of -					
	$\frac{1}{2}$	1	$1\frac{1}{2}$	2	3	4
0	0.477	0.816	0.883	0.912	0.930	0.937
0.2	.496	.817	.884	.912	.930	.937
0.4	.535	.828	.887	.913	.930	.937
0.6	.620	.847	.891	.915	.930	.937
0.8	.716	.865	.897	.917	.931	.937
0.9	.766	.872	.900	.918	.931	.937
1.1	-.860	-.839	-.754	-.747	-.727	-.743
1.2	-.535	-.556	-.527	-.517	-.496	-.505
1.6	-.138	-.208	-.214	-.214	-.207	-.206
2.0	-.047	-.091	-.118	-.119	-.114	-.115
2.4	-.018	-.054	-.073	-.079	-.079	-.079
2.8	-.009	-.030	-.046	-.053	-.056	-.056
3.2	-.004	-.017	-.030	-.038	-.041	-.042
3.6	-.002	-.011	-.020	-.027	-.032	-.033
4.0	-.001	-.007	-.014	-.020	-.025	-.027

Table 1 (b) - Nondimensional Values of Normal Component of Induced Velocity V_i/v at Azimuth Angle Ψ = 90° and 270° In Plane of a Lifting Rotor For Which $\chi = \tan^{-1} 2$ (63.45°).

r/R	V_i/v for values of Z/R of -					
	$\frac{1}{2}$	1	$1\frac{1}{2}$	2	3	4
0	0.477	0.816	0.883	0.912	0.930	0.937
0.2	.514	.737	.790	.809	.824	.834
0.4	.535	.646	.682	.704	.721	.718
0.6	.486	.517	.548	.548	.560	.556
0.8	.377	.346	.348	.363	.365	.365
0.9	-.630	-.489	-.507	-.475	-.446	-.444
1.1	-.579	-.545	-.578	-.568	-.555	-.563
1.2	-.320	-.330	-.355	-.352	-.338	-.346
1.6	-.078	-.114	-.126	-.126	-.124	-.127
2.0	-.028	-.055	-.068	-.071	-.072	-.072
2.4	-.012	-.029	-.040	-.044	-.046	-.047
2.8	-.006	-.017	-.025	-.030	-.032	-.032
3.2	-.003	-.010	-.016	-.020	-.023	-.025
3.6	-.002	-.006	-.011	-.014	-.018	-.019
4.0	0	-.004	-.008	-.010	-.013	-.014

Table 1 (c) - Nondimensional Values of Normal Component of Induced Velocity V_i/v at Azimuth Angle $\psi = 180°$ In Plane of a Lifting Rotor For Which $\chi = \tan^{-1} 2$ (63.45°).

r/R	V_i/v for values of Z/R of -					
	$\frac{1}{2}$	1	$1\frac{1}{2}$	2	3	4
0	-.459	-.145	-.070	-.038	-.017	-.009
0.2	-.506	-.181	-.079	-.043	-.019	-.010
0.4	-.517	-.216	-.091	-.049	-.020	-.011
0.6	-.506	-.251	-.100	-.054	-.022	-.011
0.8	-.470	-.282	-.112	-.060	-.023	-.012
0.9	-.452	-.293	-.121	-.063	-.024	-.012
1.1	-.403	-.307	-.132	-.070	-.026	-.013
1.2	-.369	-.307	-.137	-.073	-.027	-.014
1.6	-.209	-.298	-.156	-.087	-.030	-.015
2.0	-.009	-.240	-.162	-.096	-.033	-.017
2.4	.006	-.153	-.152	-.107	-.037	-.019
2.8	.008	-.075	-.124	-.114	-.041	-.020
3.2	.009	-.020	-.093	-.114	-.045	-.022
3.6	.004	-.002	-.057	-.105	-.048	-.024
4.0	.004	.009	-.030	-.091	-.049	-.026

Table 2 (a) - Nondimensional Values of Normal Image Component of Induced Velocity V_i/v In Plane of a Lifting Rotor at Azimuth Angle $\psi = 0°$.

r/R	V_i/v for values of Z/R of -					
	½	1	1½	2	3	4
0	-.459	-.145	-.070	-.038	-.017	-.009
0.2	-.440	-.144	-.069	-.038	-.017	-.009
0.4	-.401	-.133	-.066	-.037	-.017	-.009
0.6	-.316	-.114	-.062	-.035	-.017	-.009
0.8	-.220	-.096	-.056	-.033	-.016	-.009
0.9	-.170	-.089	-.053	-.032	-.016	-.009
1.1	-.081	-.066	-.046	-.030	-.015	-.009
1.2	-.049	-.057	-.042	-.028	-.015	-.009
1.6	.019	-.025	-.028	-.022	-.013	-.008
2.0	.027	.006	-.017	-.016	-.011	-.008
2.4	.022	.004	-.009	-.011	-.010	-.007
2.8	.017	.008	-.003	-.007	-.008	-.006
3.2	.012	.010	-.004	-.004	-.006	-.005
3.6	.009	.008	.002	-.001	-.005	-.004
4.0	.007	.007	.003	.000	-.004	-.004

Table 2 (b) - Nondimensional Values of Normal Image Component of Induced Velocity V_i/v In Plane of a Lifting Rotor at Azimuth Angle $\psi = 90°$ and $270°$.

r/R	V_i/v for values of Z/R of -					
	$\frac{1}{2}$	1	$1\frac{1}{2}$	2	3	4
0	-.459	-.145	-.070	-.038	-.017	-.009
0.2	-.370	-.116	-.059	-.034	-.016	-.009
0.4	-.262	-.092	-.049	-.030	-.014	-.008
0.6	-.162	-.069	-.040	-.024	-.013	-.008
0.8	-.087	-.050	-.032	-.022	-.012	-.007
0.9	-.059	-.040	-.029	-.020	-.011	-.007
1.1	-.016	-.029	-.024	-.017	-.010	-.006
1.2	-.003	-.023	-.021	-.016	-.010	-.006
1.6	.020	-.006	-.012	-.010	-.008	-.005
2.0	.021	.002	-.006	-.007	-.006	-.004
2.4	.017	.005	-.002	-.004	-.005	-.004
2.8	.012	.006	.001	-.002	-.003	-.003
3.2	.009	.006	.002	.000	-.002	-.002
3.6	.007	.006	.003	.001	-.002	-.002
4.0	.006	.005	.003	.001	-.001	-.001

Table 2 (c) - Nondimensional Values of Normal Image Component of Induced Velocity V_i/v In Plane of a Lifting Rotor at Azimuth Angle $\Psi = 180°$.

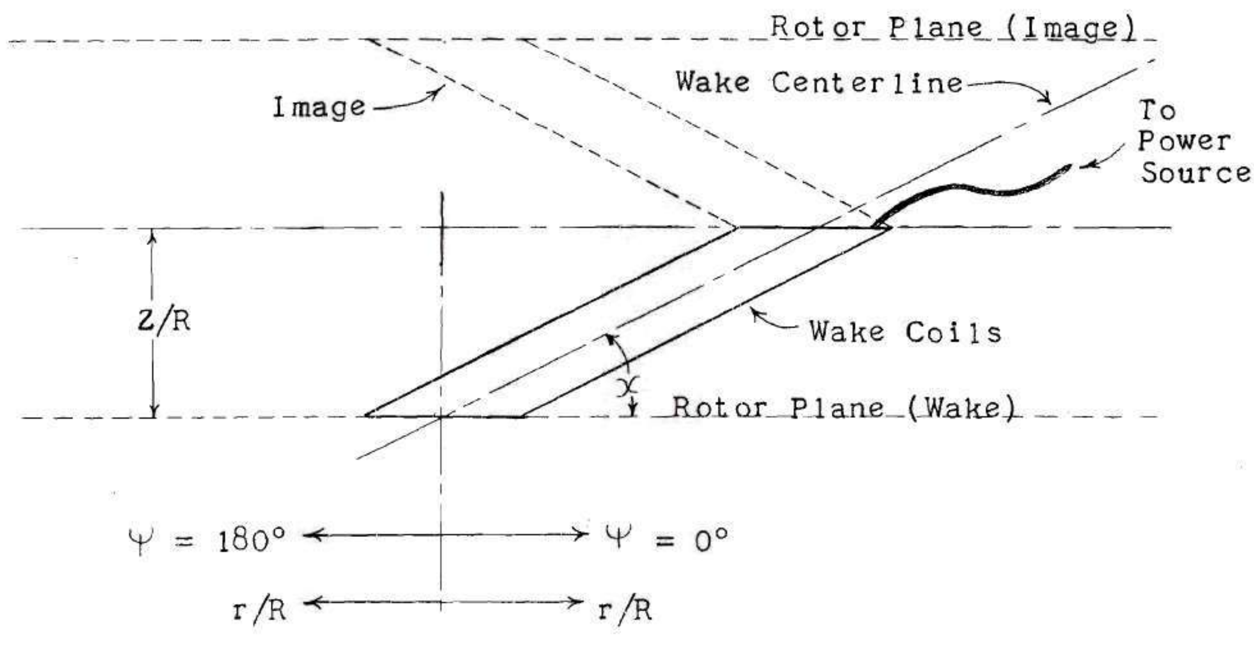

Figure 1 - Wake Model Arrangement

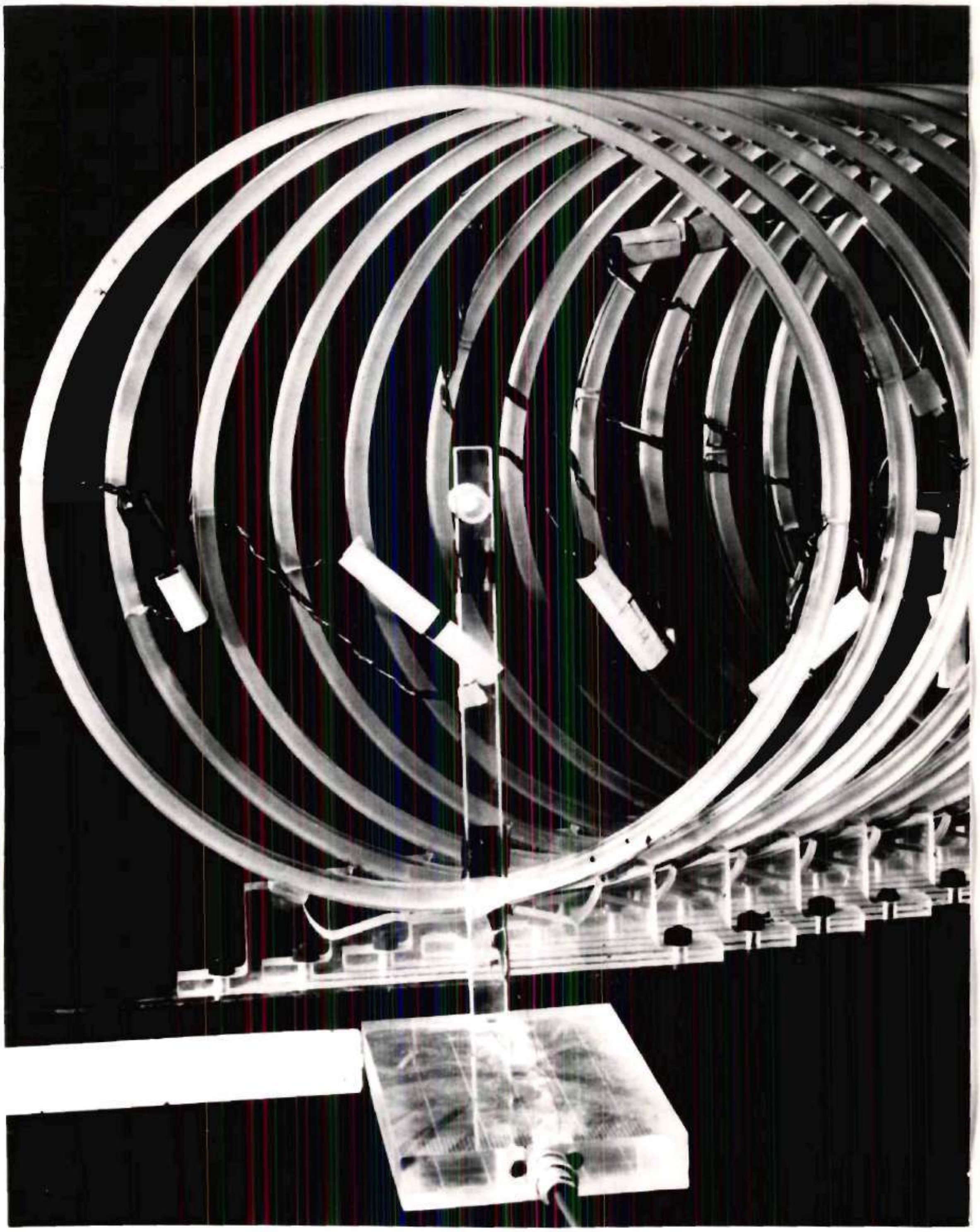

(a) View A

Figure 2 - Electromagnetic-analogy Model Assembly.

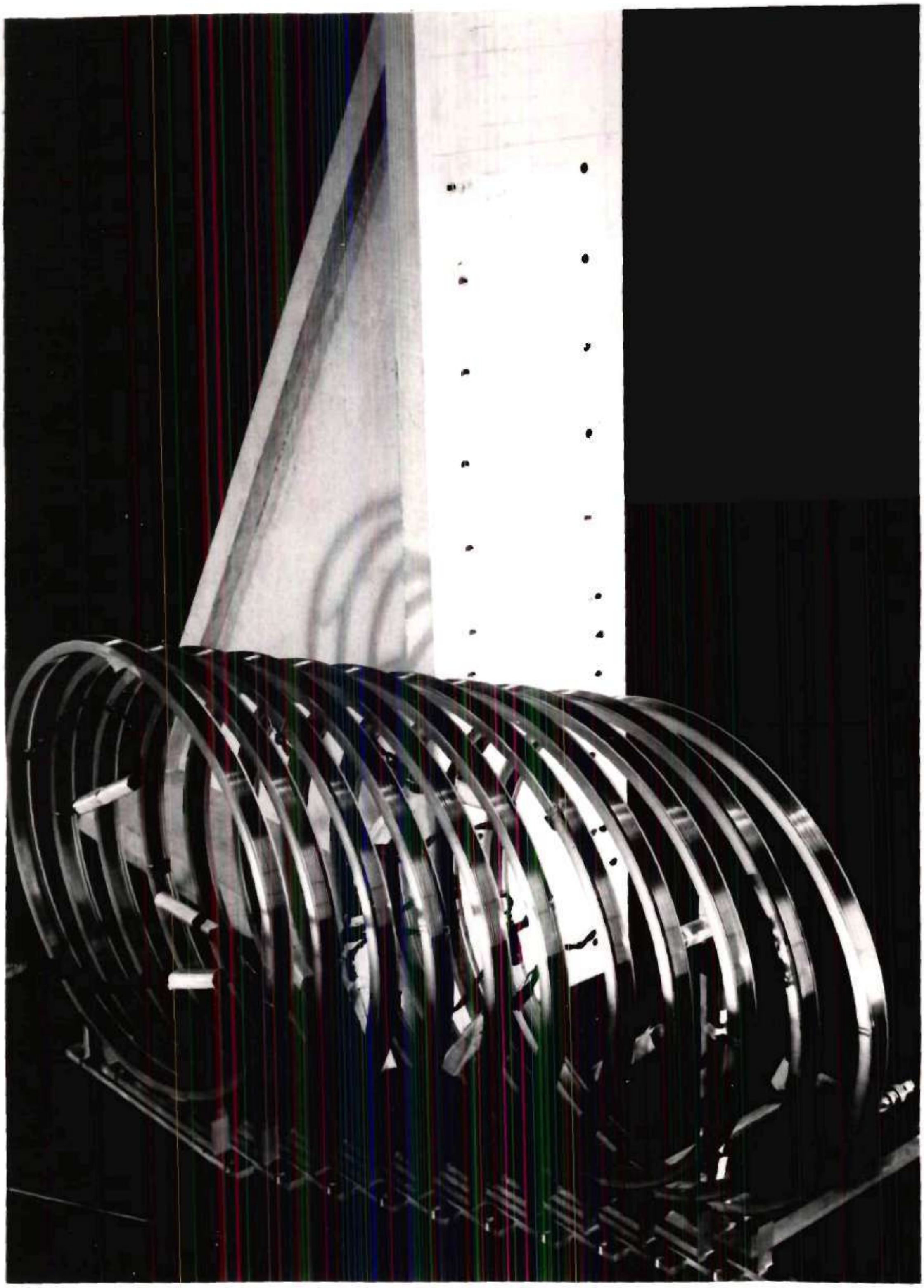

View B

Figure 2 - Continued

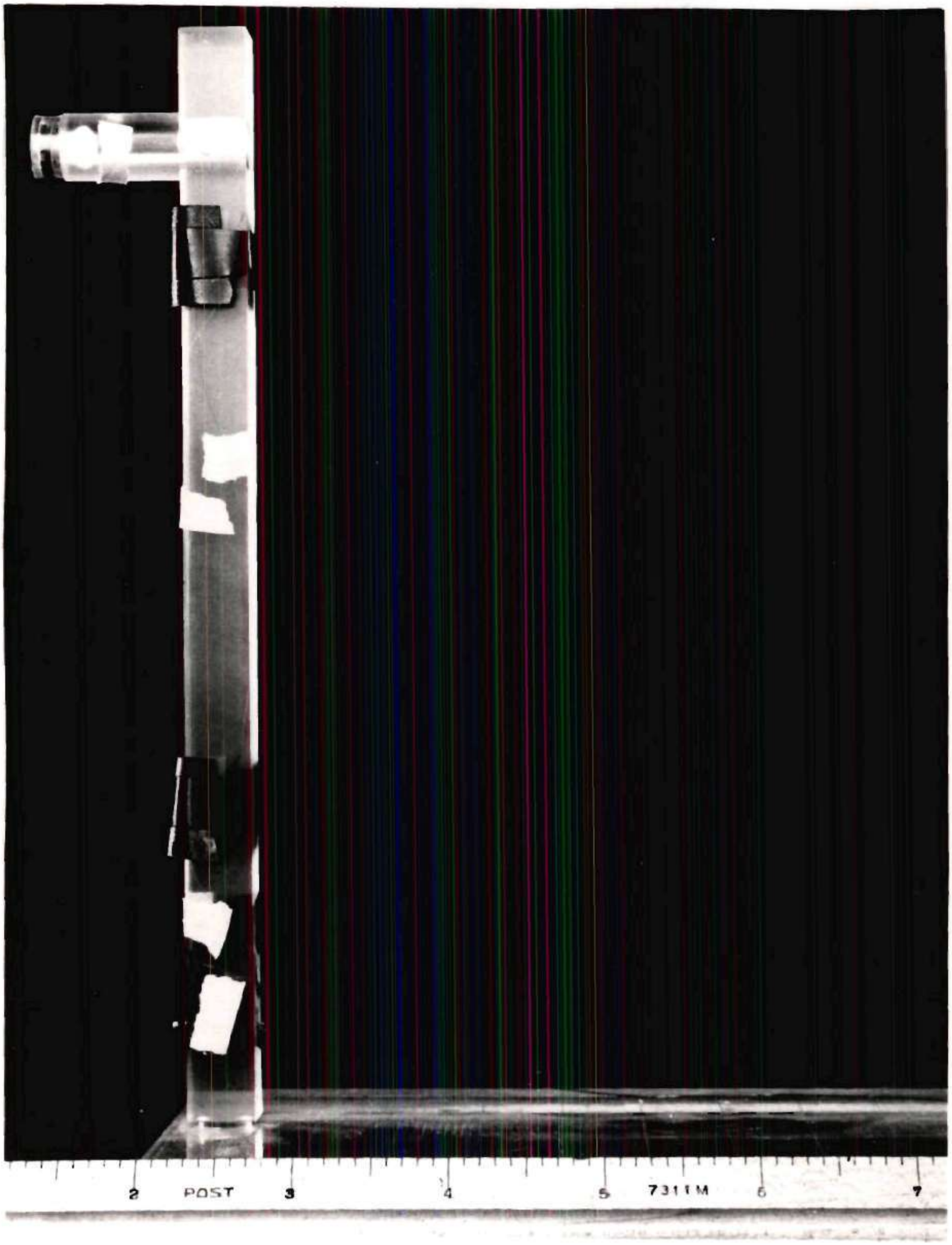

Figure 3 - Search Coil Assembly.

Figure 4 - Fixed Frequency Amplifier and Indicator Unit.

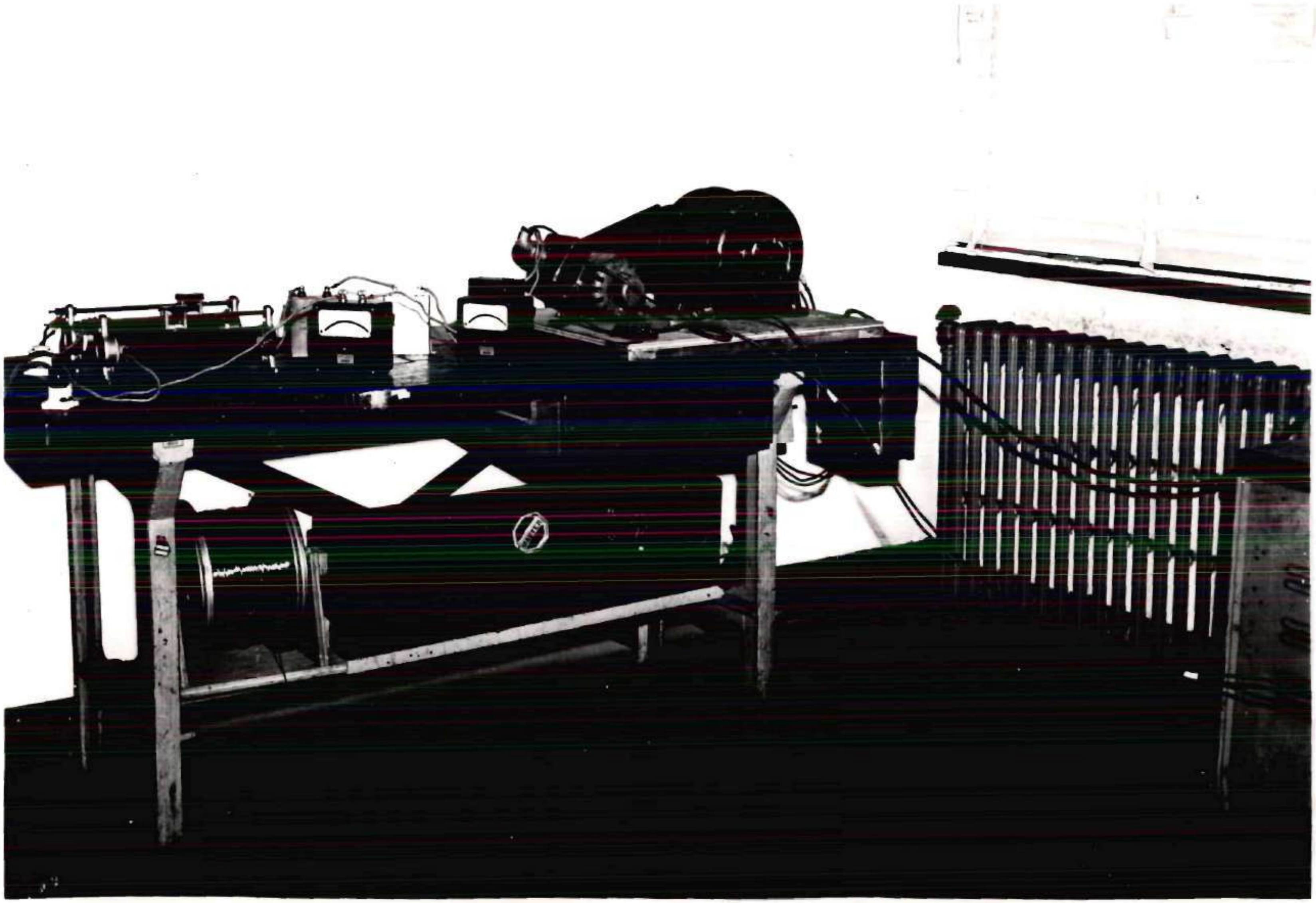

Figure 5 - Power Supply Assembly.

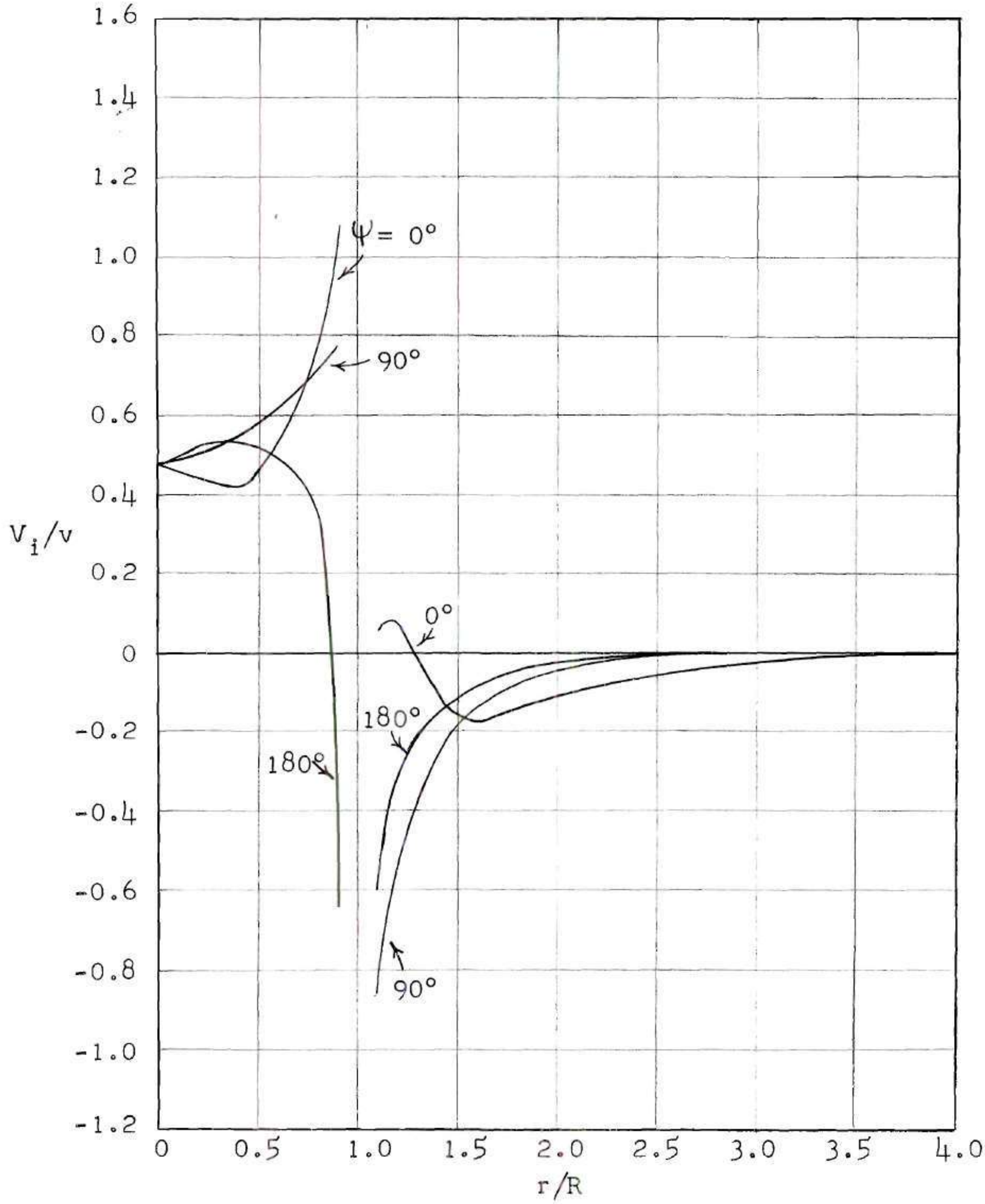

(a) For Nondimensional Ground Distance Z/R = 0.5

Figure 6 - Variation of Nondimensional Normal Component of Induced Velocity Along the Radius.

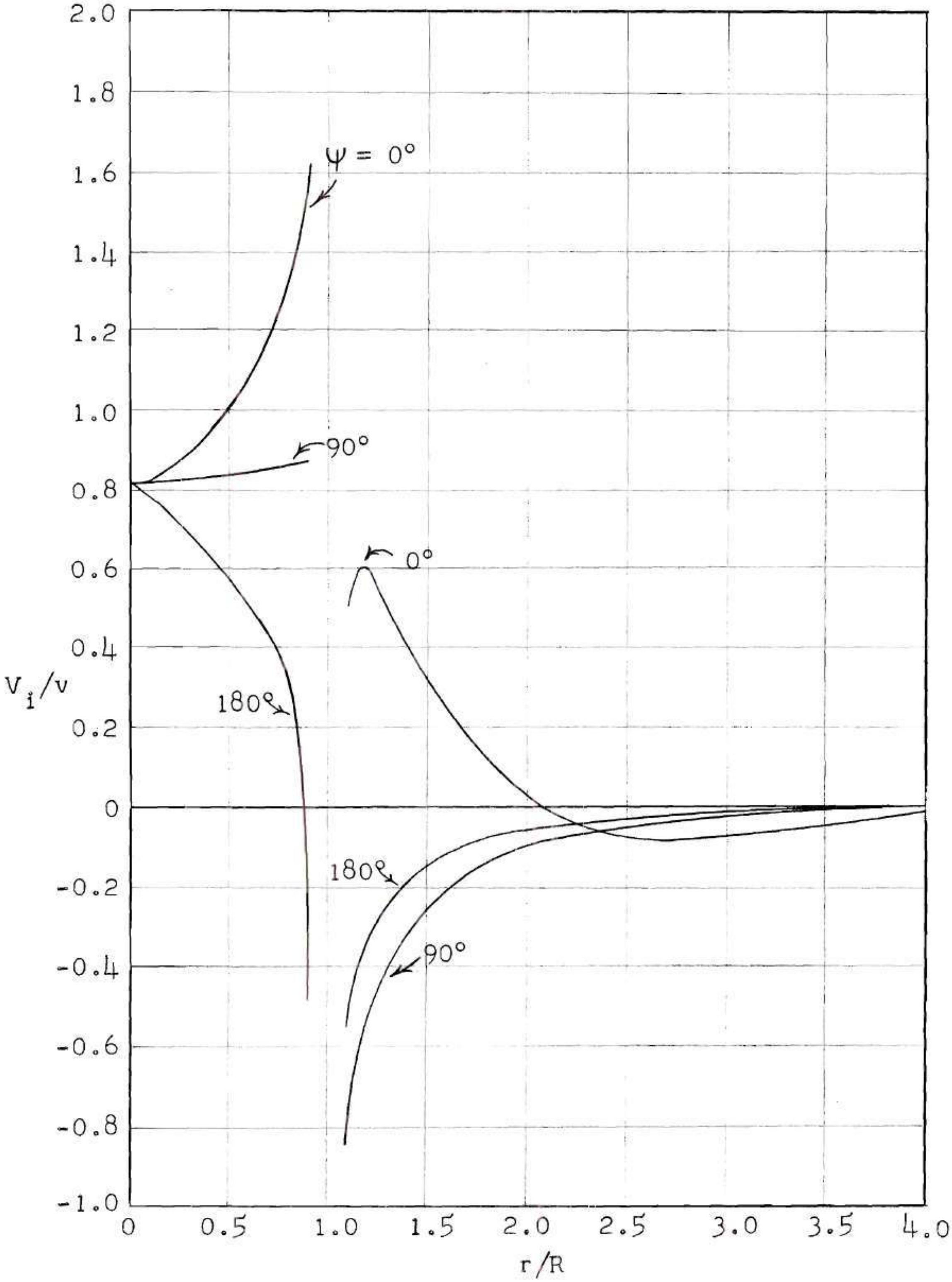

(b) For Nondimensional Ground Distance Z/R = 1.0

Figure 6 - Continued

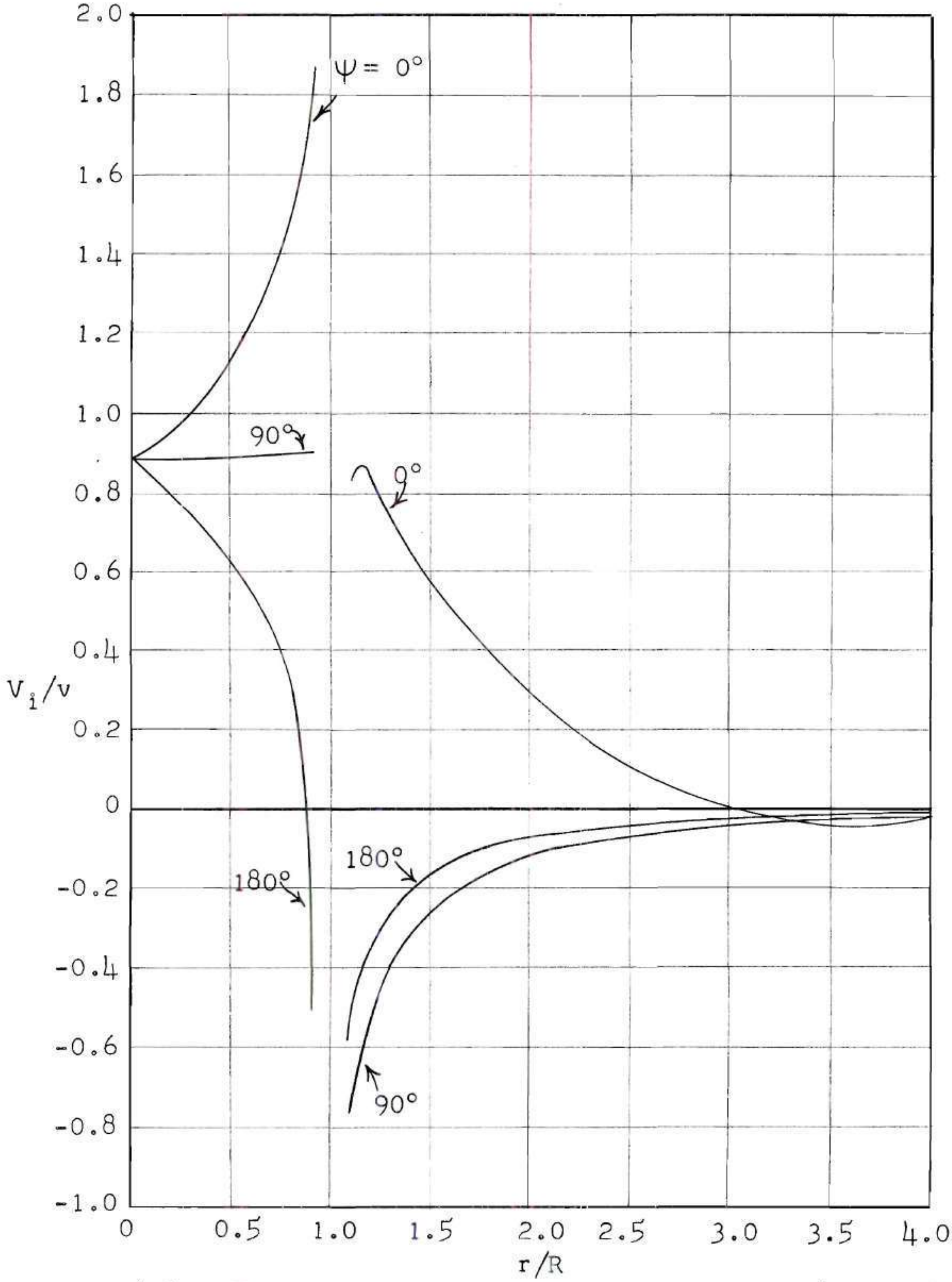

(c) For Nondimensional Ground Distance Z/R = 1.5

Figure 6 - Continued

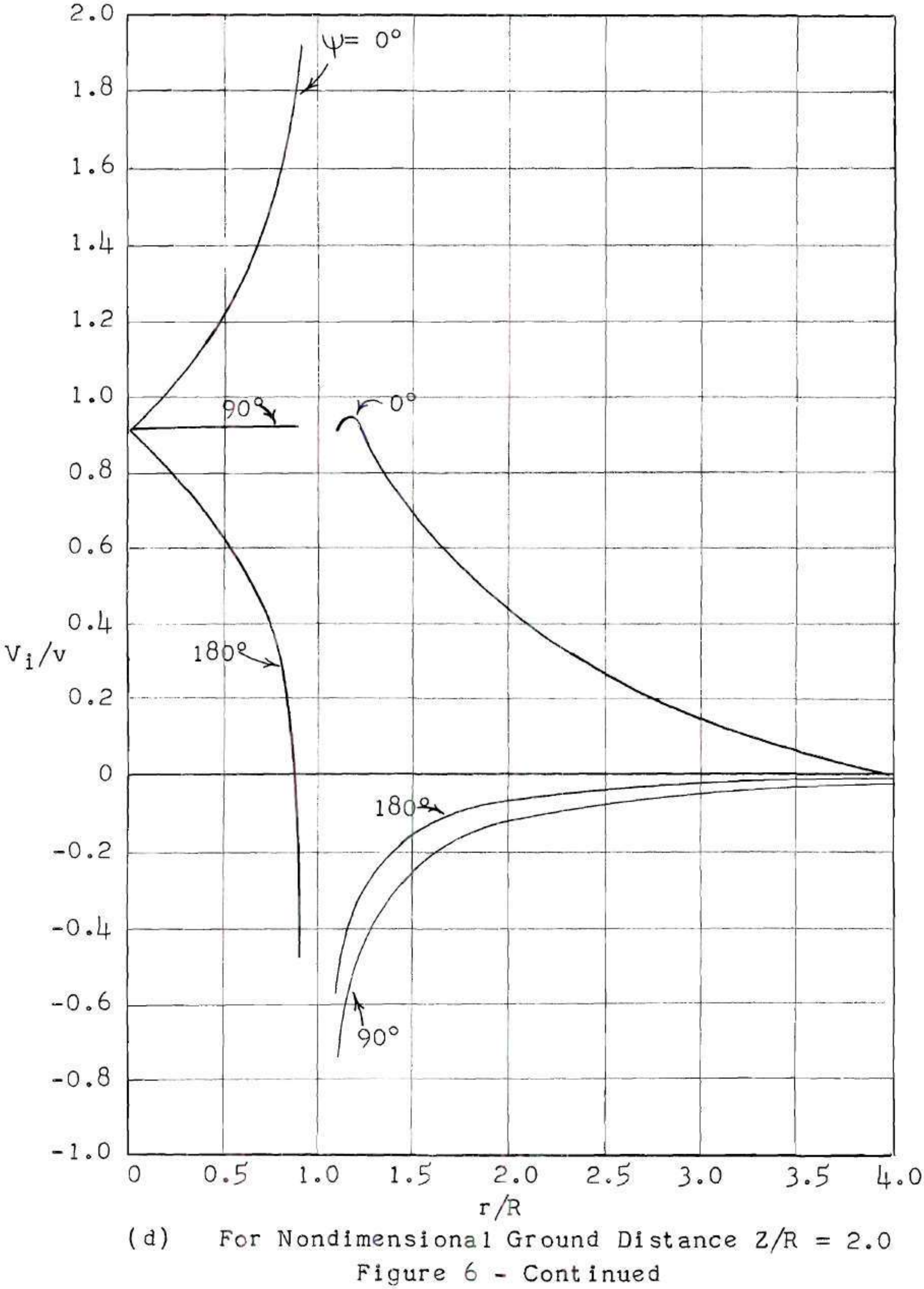

(d) For Nondimensional Ground Distance Z/R = 2.0

Figure 6 - Continued

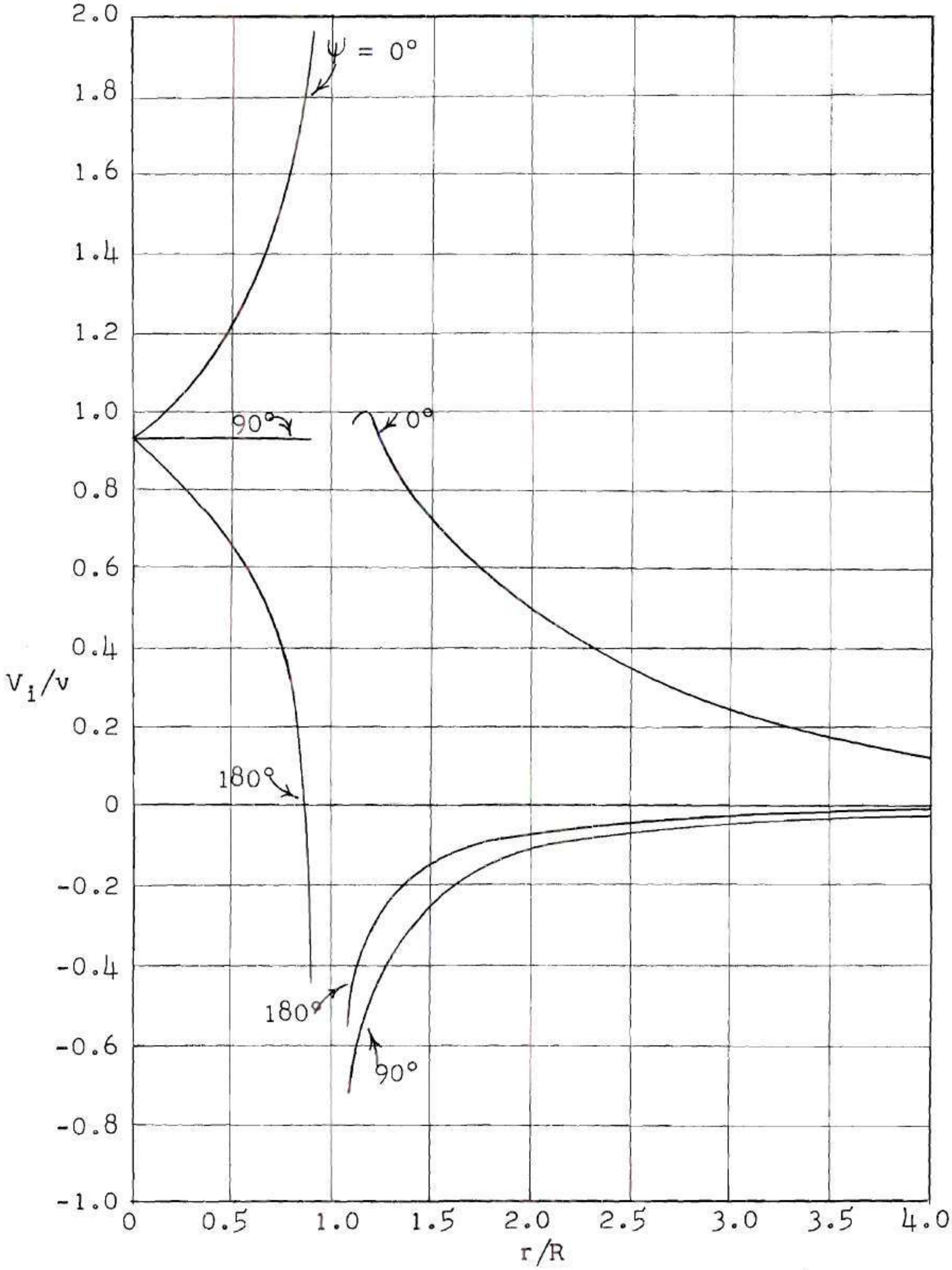

(e) For Nondimensional Ground Distance Z/R = 3.0

Figure 6 - Continued

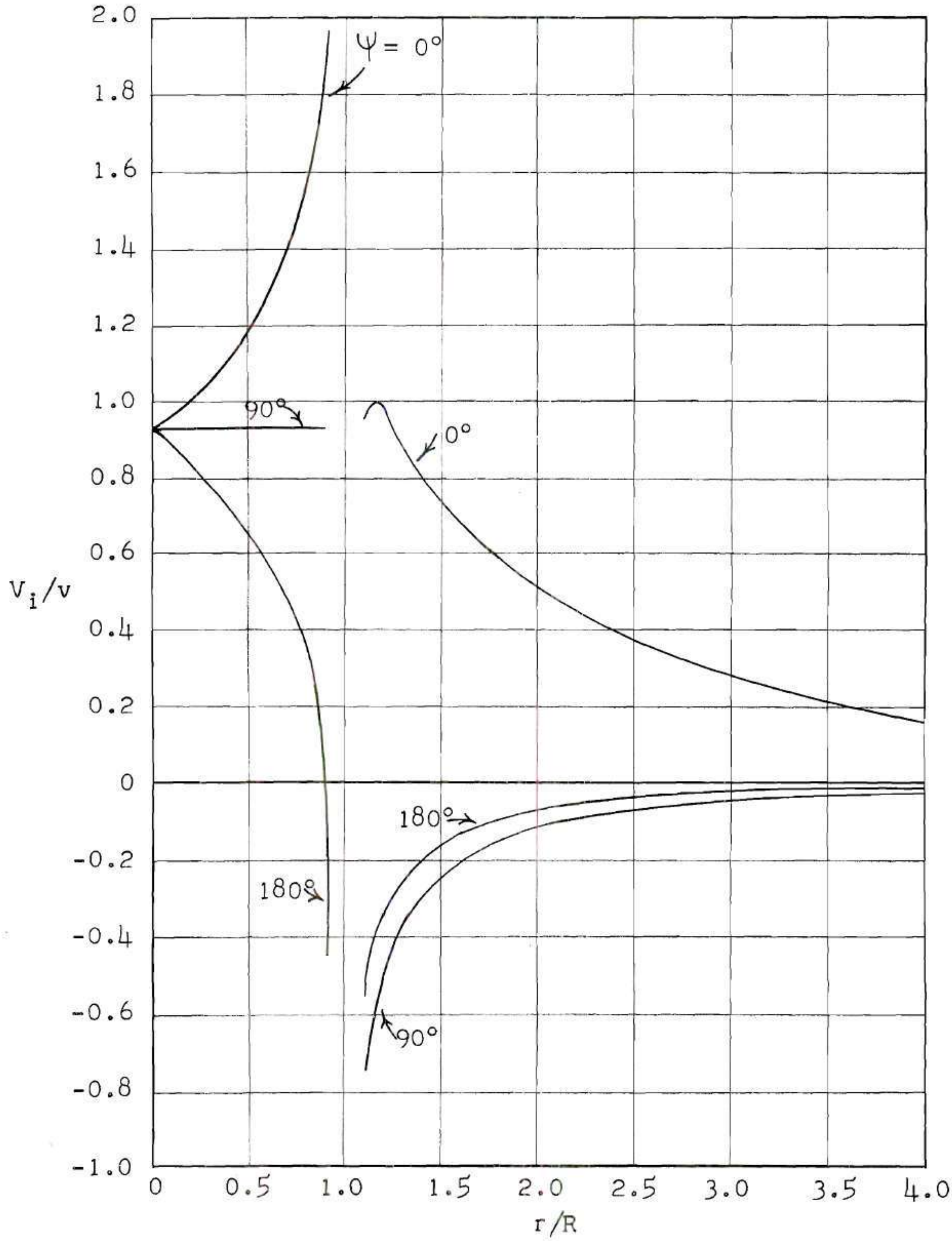

(f) For Nondimensional Ground Distance Z/R = 4.0

Figure 6 - Continued

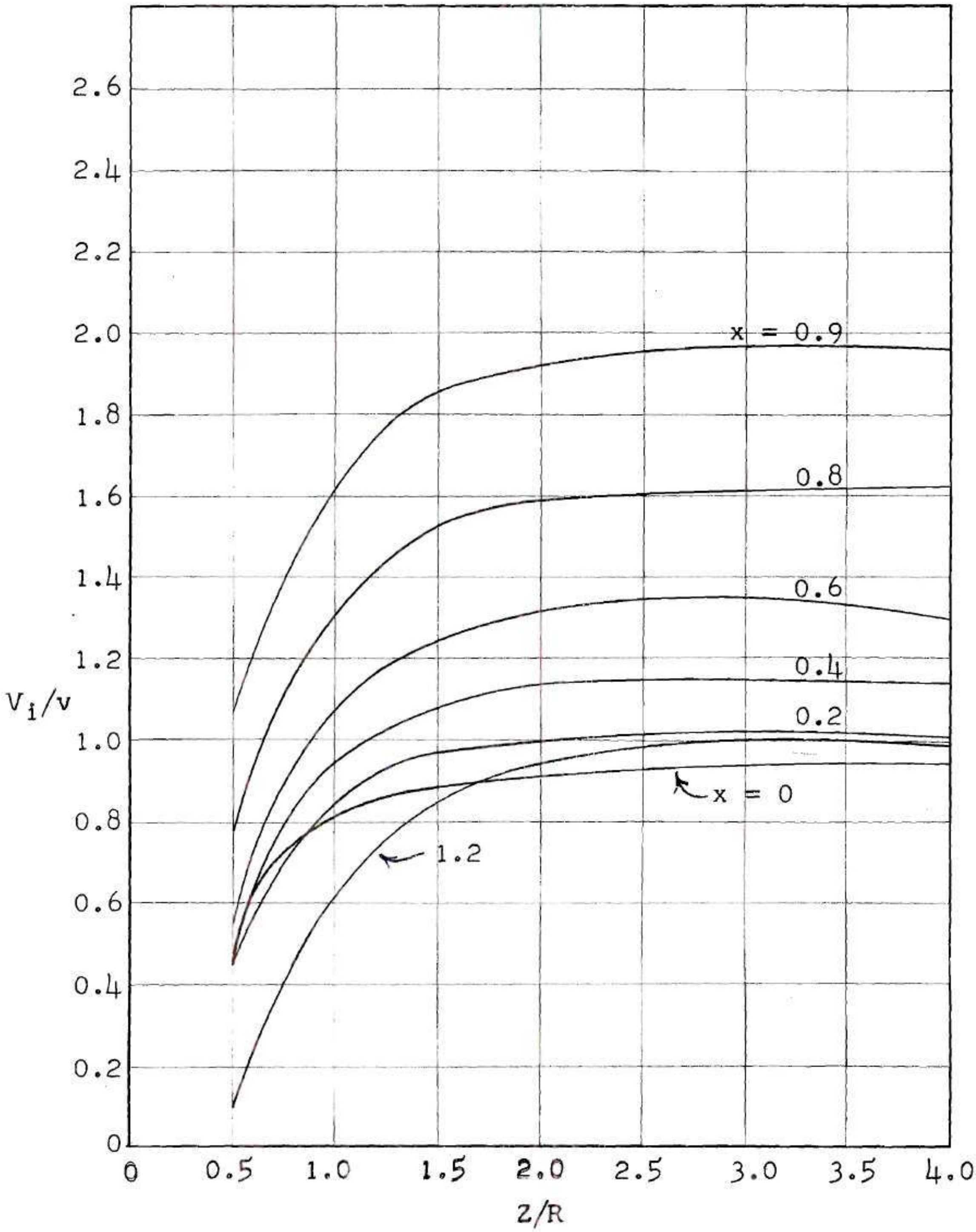

(a) For Azimuth Angle ψ = 0°

Figure 7 - Variation of Nondimensional Normal Component of Induced Velocity With Ground Distance.

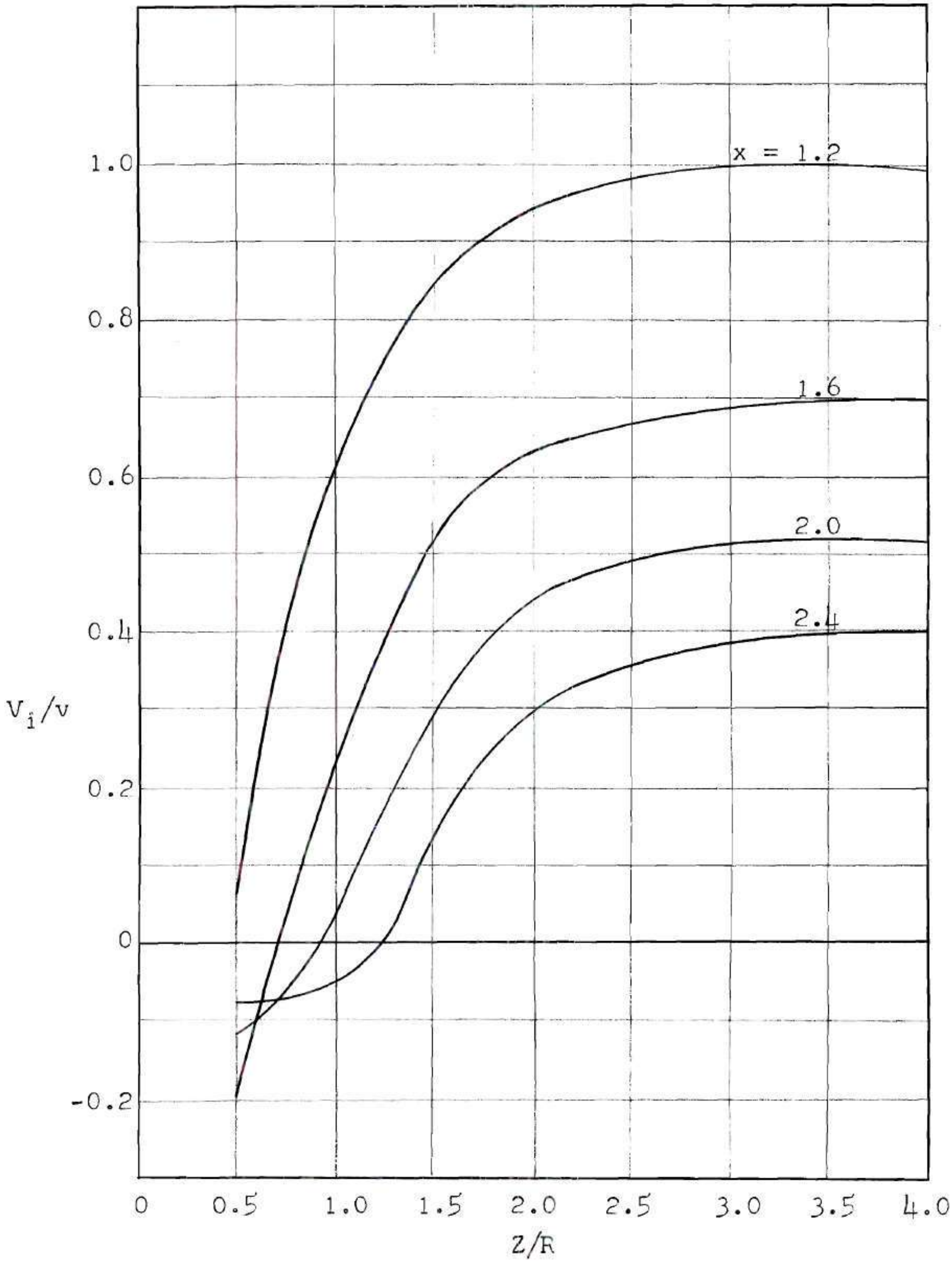

Figure 7 (a) - Continued

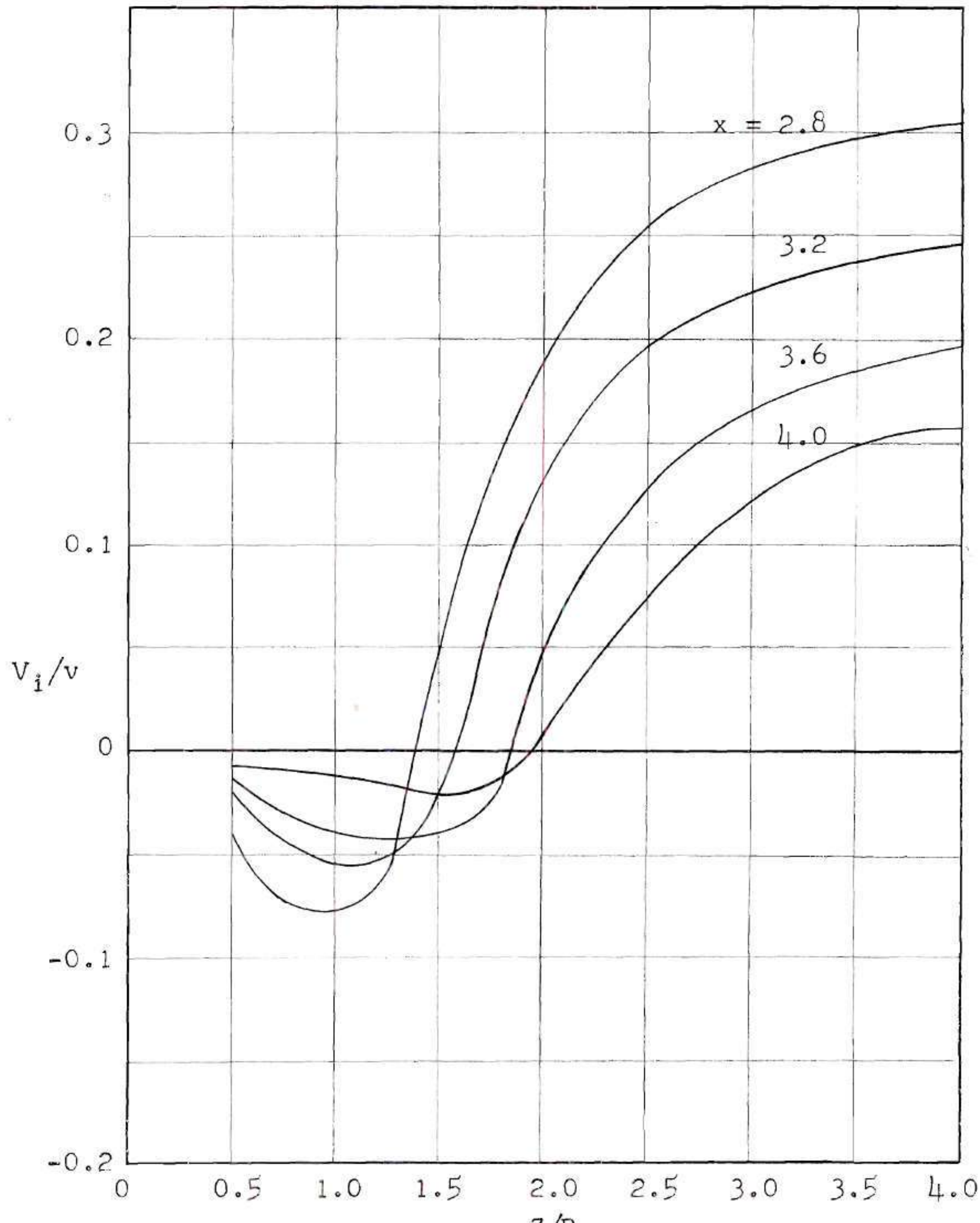

Figure 7 (a) - Continued

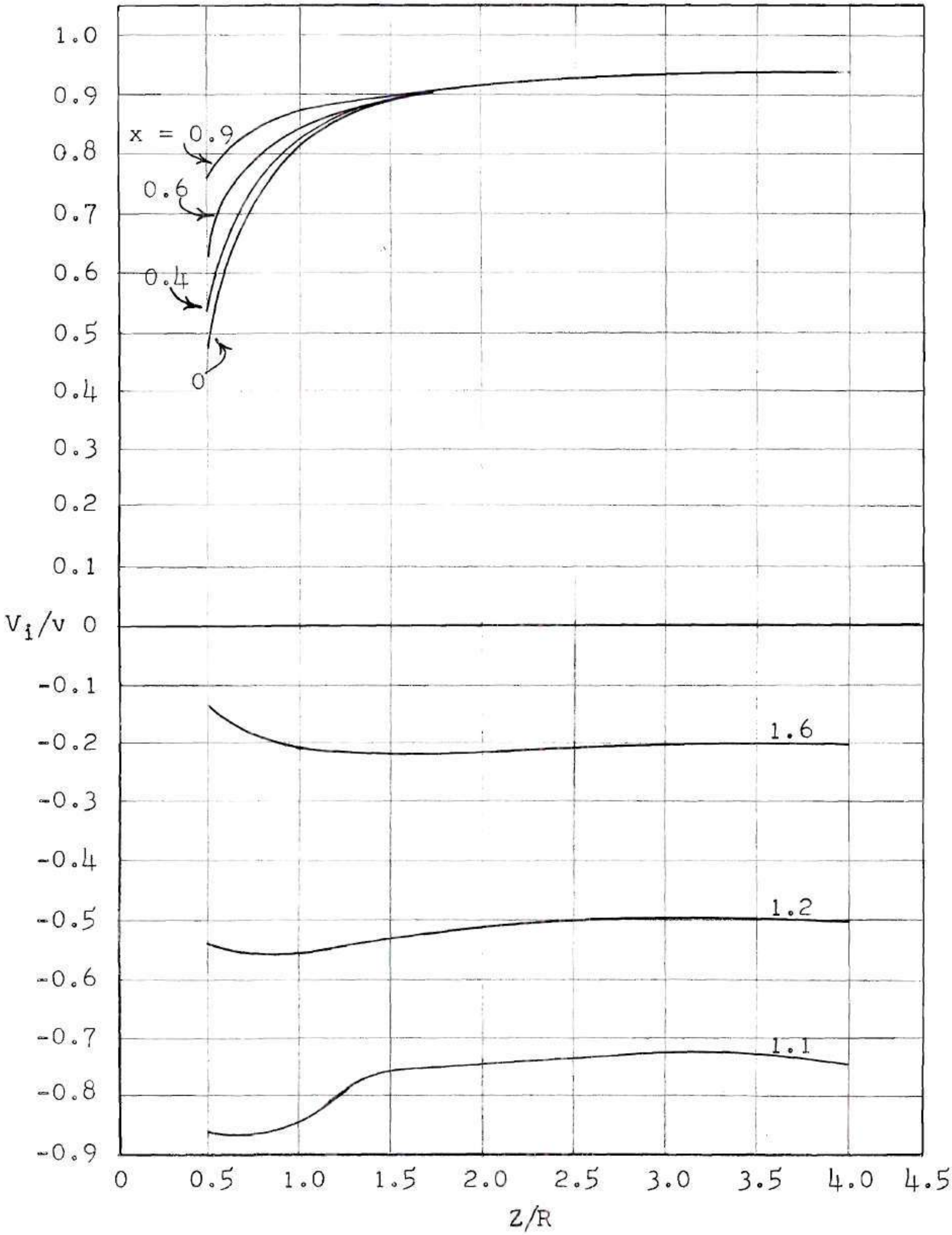

(b) For Azimuth Angle ψ = 90°

Figure 7 - Continued

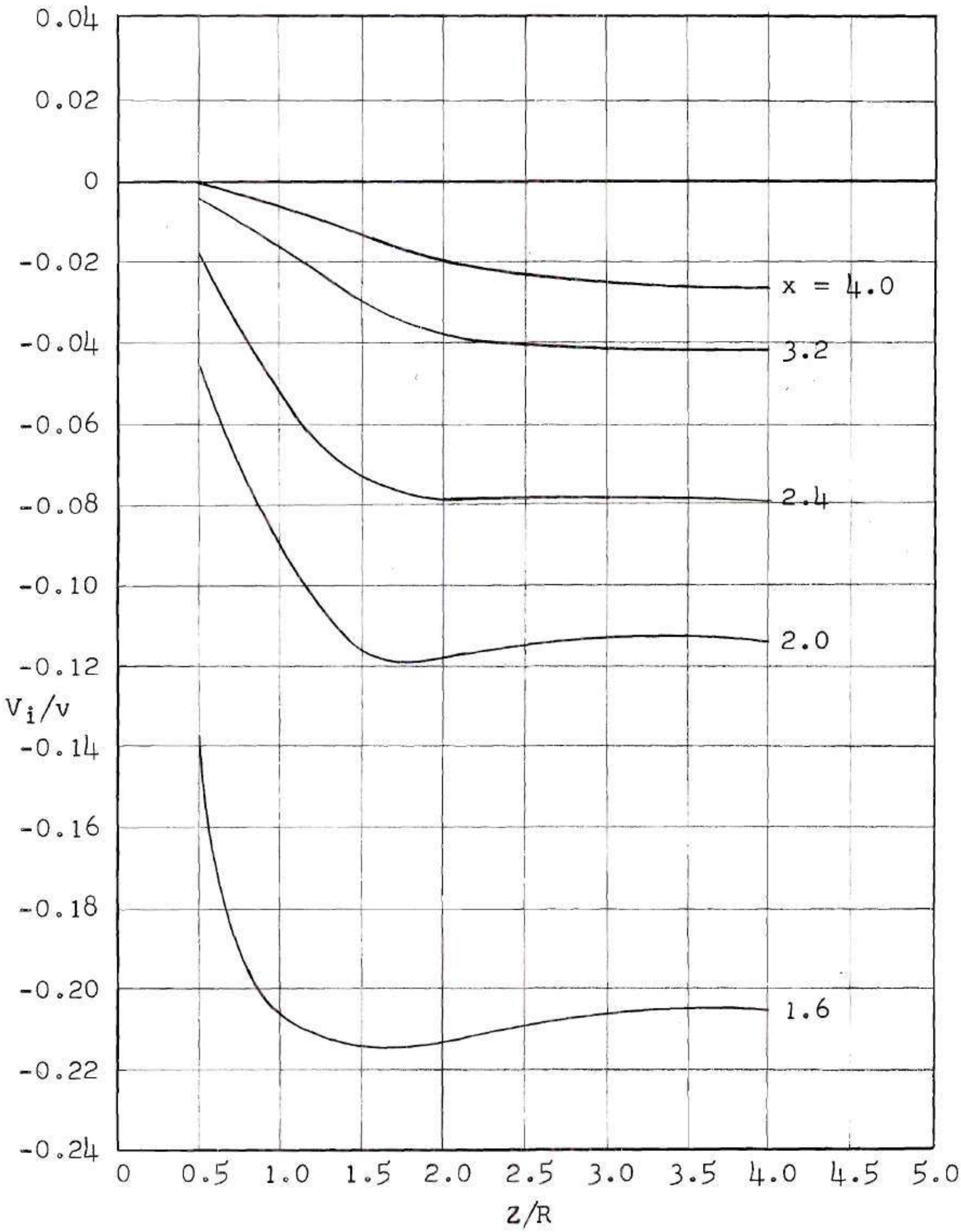

Figure 7 (b) - Continued

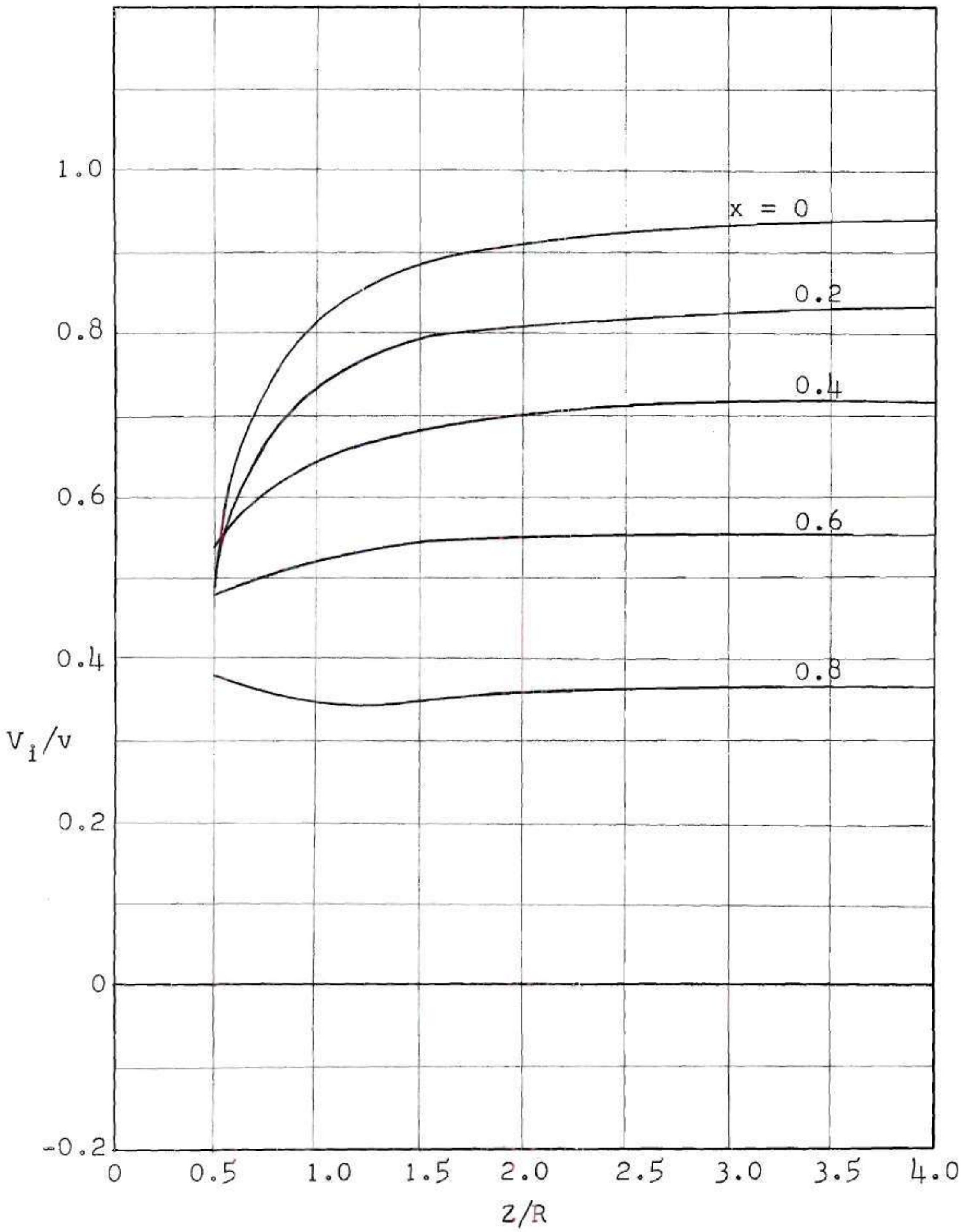

(c) For Azimuth Angle ψ = 180°

Figure 7 - Continued

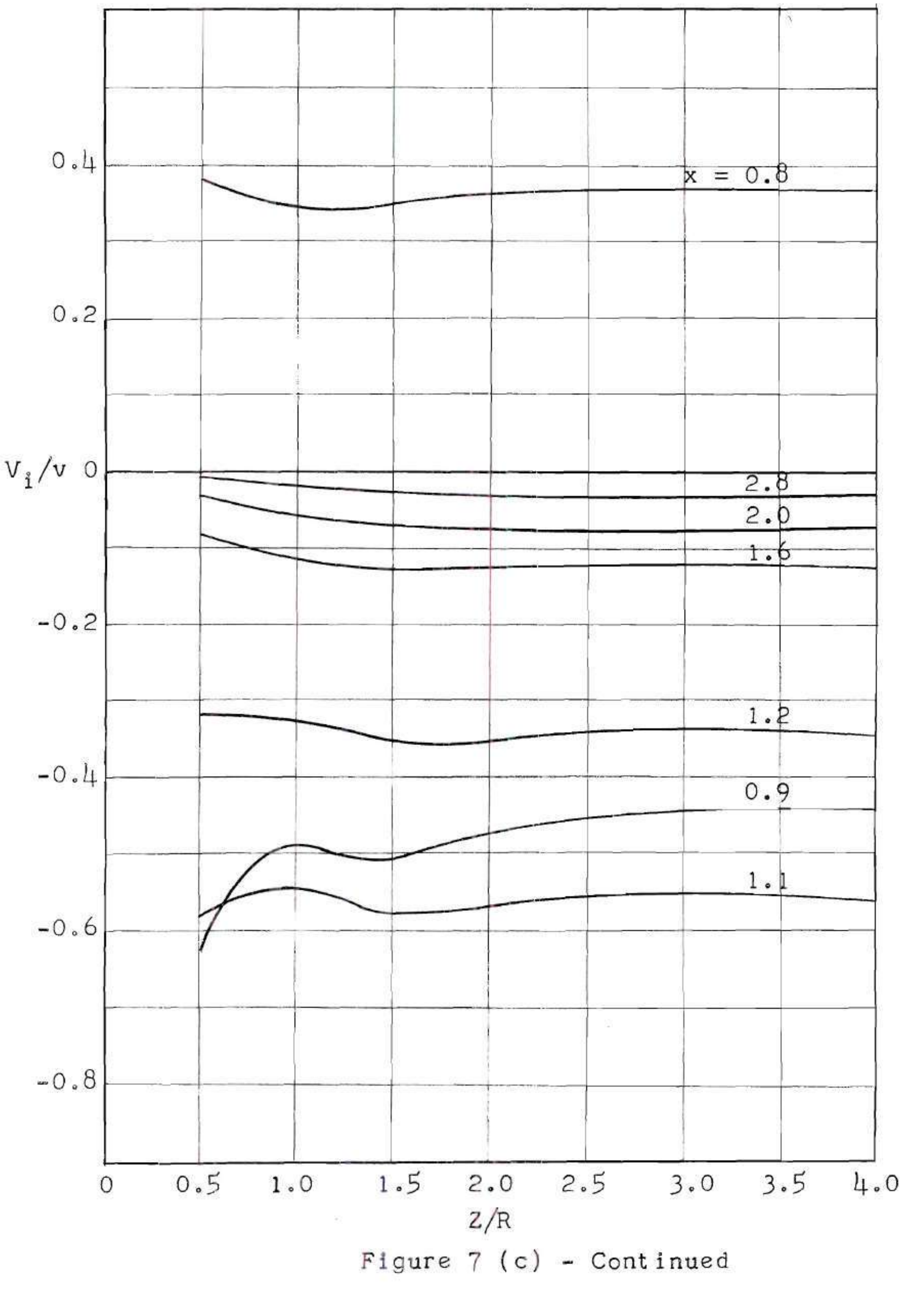

Figure 7 (c) - Continued

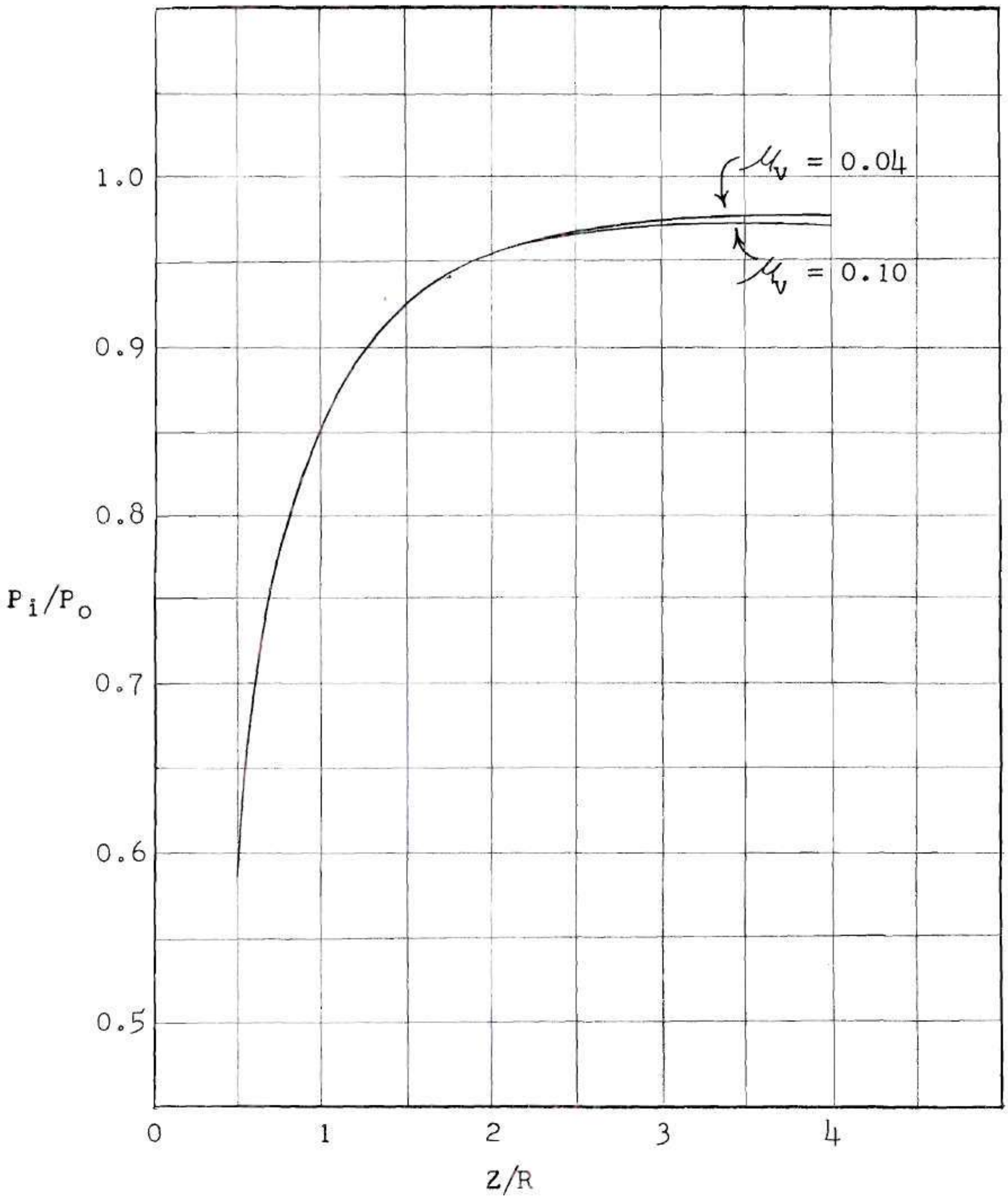

Figure 8 - Variation of Induced Power Ratio With Distance Above Ground Plane.

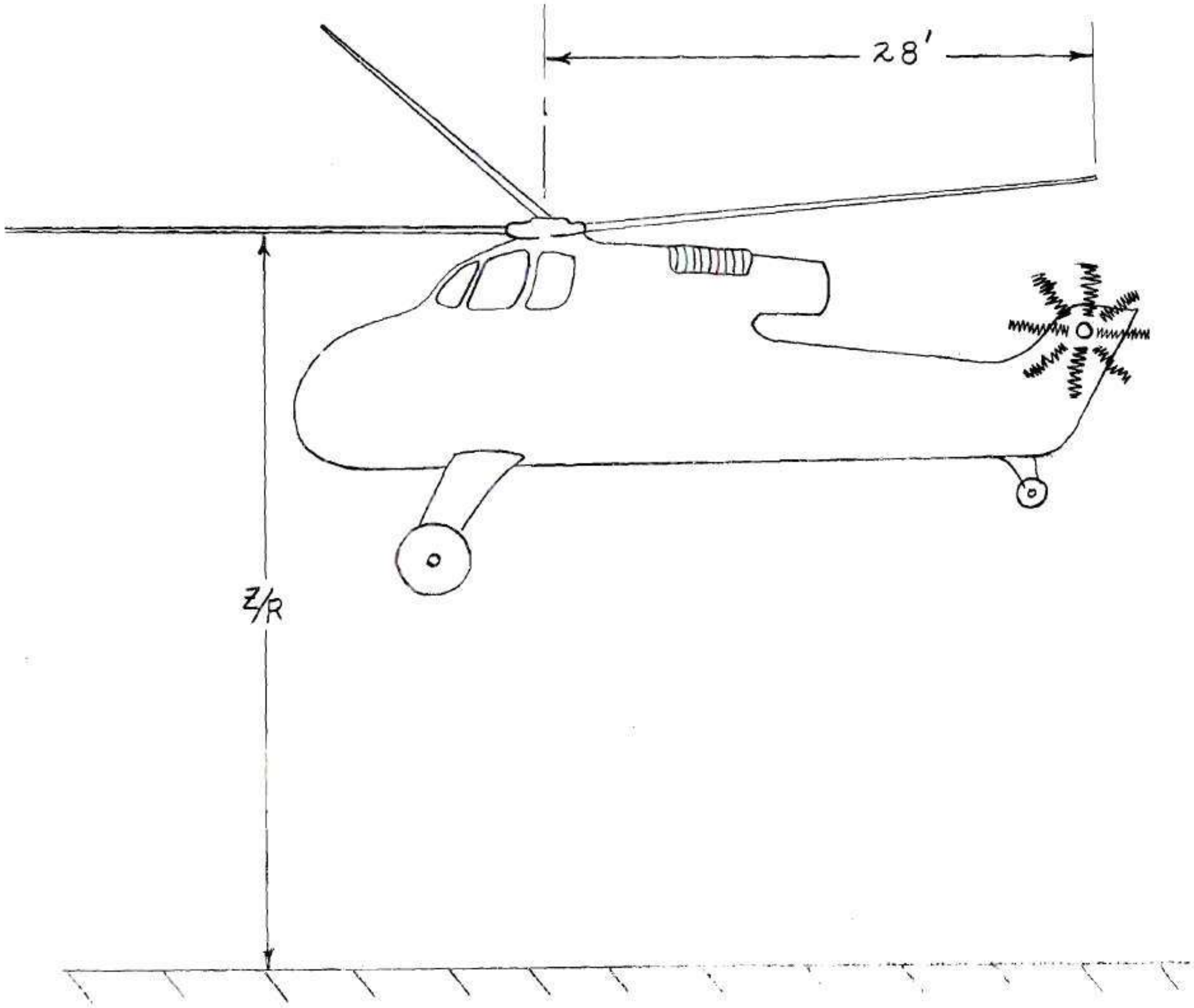

Figure 9 - Representative Helicopter With Dimensions Used in Sample Problem.

BIBLIOGRAPHY

1. Swanson, Robert S., *An Electromagnetic-Analogy Method of Solving Lifting-Surface-Theory Problems*, National Advisory Committee For Aeronautics, Wartime Report L-120, 1945.

2. Castles, Walter, Jr., Durham, Howard L., Jr., and Kevorkian, Jiriar, *Normal Component of Induced Velocity For Entire Field of a Uniformly Loaded Lifting Rotor With Highly Swept Wake As Determined by Electromagnetic Analog*, National Advisory Committee For Aeronautics, Technical Note 4238, 1958.

3. Drees, Meijer, Jr., "A Theory of Airflow Through Rotors and Its Application to Some Helicopter Problems", *The Journal of the Helicopter Association of Great Britain*, Volume III, No. 2, July-August-September, 1949, pages 79 - 104.

4. Castles, Walter, Jr., and De Leeuw, Jacob Henri, *The Normal Component of the Induced Velocity of a Lifting Rotor and Some Examples of Its Application*, National Advisory Committee For Aeronautics, Report 1184, 1954.

5. Kuchemann, Kietrich, and Weber, Johanna, *Aerodynamics of Propulsion*, New York: McGraw Hill Book Company, 1953, page 306.